SciEn
Proceedings of 8th International Conference on Mechanical Engineering and Renewable Energy 2025
10-12 December, 2025, Chattogram, BANGLADESH
SciEn Conference Series: Engineering Vol. 4, 2026, pp 667-672 https://doi.org/10.38032/scse.2026.4.303

Energy and Exergy Analysis of Recuperative Organic Rankine Cycle for Six Low-GWP Refrigerants

Mostafizur Rahaman[1], Khaza Shahriar[1], and Mohammad Ariful Islam[2,]*

[1]Department of Energy Science and Engineering, Khulna University of Engineering & Technology, Khulna-9203, Bangladesh
[2]Department of Mechanical Engineering, Khulna University of Engineering & Technology, Khulna-9203, Bangladesh

ABSTRACT

The need to recover waste heat from industrial operations is highlighted by the growing need for sustainable energy solutions worldwide. This heat is frequently wasted, which reduces system effectiveness and deteriorates environmental effects. A thorough thermodynamic analysis of recuperative organic Rankine Cycles (ORCs) using low-GWP (GWP < 10) environment-friendly refrigerants is presented in this work. A numerical simulation for six low-GWP refrigerants: R-1243zf, R-1234yf, R-1233zd(E), R-1224yd(Z), R-1234ze(E), and R-1336mzz(Z) is conducted using the Python programming language. In this study, the effects of pump inlet pressure (0.8-1.5 MPa) and turbine inlet pressure (1.0-2.0 MPa) on system performance are evaluated using mass, entropy, energy, and exergy balance equations. R-1243zf emerges as the optimal refrigerant choice for recuperative ORC systems, offering the best combination of high power output (28.04 kW), excellent thermal efficiency (9.43%), and superior exergetic efficiency (31.00%), making it most suitable for applications prioritizing maximum power generation.

Keywords: Energy, Exergy, Organic Rankine Cycle (ORC), Refrigerants, Global Warming Potential (GWP).

1. Introduction

Due to the fact that thermal systems operate with efficiency well below 100%, a great amount of waste heat is produced as flue gas that, if discarded in the environment, is a source of pollution [1]. Therefore, utilizing various waste heat recovery (WHR) systems can help in restoring a large portion of the lost energy, thereby improving the overall efficiency of the system and reducing both carbon emissions and environmental pollution [2]. Over the years, a variety of WHR techniques have been established, including refrigeration and heat pump systems, steam Rankine cycle, thermoelectric generators, Organic Rankine Cycle (ORC), heat pipe, thermal wheel, etc. [3]. Among these, ORC has emerged as one of the most prominent and key focus areas for researchers in the field of WHR in recent decades [4], mainly due to its capability of operating with moderate to low-temperature waste heat, simpler maintenance, and better flexibility [5, 6]. Furthermore, working fluids have a great impact on the performance of ORC [7], and the search for appropriate working fluids in recent decades has shifted towards low-GWP refrigerants due to international protocols concerning ozone depletion and global warming [8]. For instance, Tan et al. did an experimental investigation of an ORC-VCR system and found a maximum capacity of cooling is 2.1 kW with a COP of 0.175 [9]. Similarly, Hu et al. [7] used computer-based molecular design for selecting working fluids of single-pressure and dual-pressure evaporative ORC systems, and they found that R1345yf(Z) and R1381yf refrigerants are the best performers for both systems. Moreover, Bahrami et al. [8] assessed low-GWP refrigerant performance through a literature review and suggested that R-1233zd(E), R-1366mzz(Z), and R-1234ze(Z) have great potential among the low-GWP HFOs. In addition, Grauberger et al. first simulated an Organic Rankine–Vapor Compression (ORVC) prototype using Engineering Equation Solver (EES) and later built the system to test and validate the low-GWP refrigerant R1234ze(E). Likewise, Tanbar et al. [10] conducted economic and thermodynamic analyses of a binary cycle ORC and binary cycle ORC recuperator system using low-GWP working fluids R1233zd(E), R1234z(Z), R1234ze(E), R1243zf, R1224yd(Z), and R1234yf in the case of expanded steam of about 100°C from an Indonesian geothermal power plant. They found that the recuperator system using the working fluid R1233zd(E) performed best in terms of output and efficiency, with an efficiency of about 10% and an output of about 2200 kW. Finally, a thermodynamic analysis of a direct vapor generation ORC system with low-GWP working fluids was carried out by Jiang et al. [11]. They did optimization with power output as the objective parameter and found that the refrigerant R245ca produced the highest power output, while the refrigerant R1336mzz(Z) exhibited the best result in terms of efficiency. They concluded R1336mzz(Z) as the most promising working fluid for direct vapor generation ORC.

According to the literature study, there hasn't been a comprehensive evaluation of the performance of some low-GWP refrigerants for the recuperative ORC cycle. The present study object to investigate the thermodynamic performance of recuperative ORC for six low-GWP refrigerants: R1234yf, R1234ze(E), R1243zf, R1224yd(Z), R1336mzz(Z) , and R1233zd(E) in terms of net work output, total exergy destruction, energy, and exergy efficiency.

2. Methodology

This investigation is presented as a methodology with four steps to analyze recuperative ORC for low global warming potential (GWP) refrigerants, shown in Fig. 1. In the first step, mathematical modeling of recuperative ORC is developed using fundamental thermodynamic principles (mass, energy, entropy, and exergy balance equations). In the second step, six low-GWP (GWP < 10) and zero ozone-depletion potential (ODP) refrigerants are selected, including R1243zf, R1234ze(E), R1234yf, R1233zd(E), R1224yd(Z), and R1336mmz(Z). In the next step, a detailed parametric investigation to assess how the critical process variables (evaporating and condensing pressures) affect the system's performance parameters. In the final step, system performance is evaluated through key thermodynamic parameters such as net work output, total exergy destruction, thermal efficiency, and exergy efficiency.

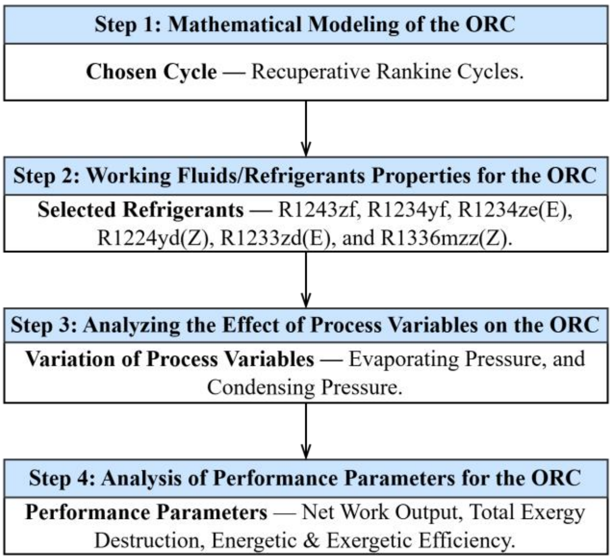

Fig. 1: Methodology for the analysis of recuperative ORC

2.1 Mathematical Modeling

Energy and Exergy analysis of the recuperative ORC is conducted through comprehensive mathematical modeling using fundamental balance equations in this section. The Recuperative Organic Rankine Cycle (RORC) enhances the basic ORC by adding a recuperator to recover heat from the turbine exhaust, improving overall efficiency. As shown in Fig. 2a, it includes five components, such as a pump, turbine, evaporator, recuperator, and condenser operating in a closed loop. The working fluid is pressurized by the pump (1-2), preheated in the recuperator (2-2a), and fully vaporized in the evaporator (2a-3). Then vapor expands through the turbine (3-4), producing work, then transfers residual heat in the recuperator (4-4a) before condensing back to liquid in the condenser (4a-1). Also, the T-s diagram of the ORC system is shown in Fig. 2b.

The mathematical modeling is done by using mass balance equations (MBE), entropy balance equations (EnBE), energy balance equations (EBE), and exergy balance equations (ExBE) for each component of the system. Finally, system performance is evaluated through total work output ($\dot{W}_{out}$), total exergy destruction ($\dot{E}_{dest}$), energetic efficiency (η_{en}), and exergetic efficiency (η_{ex}).

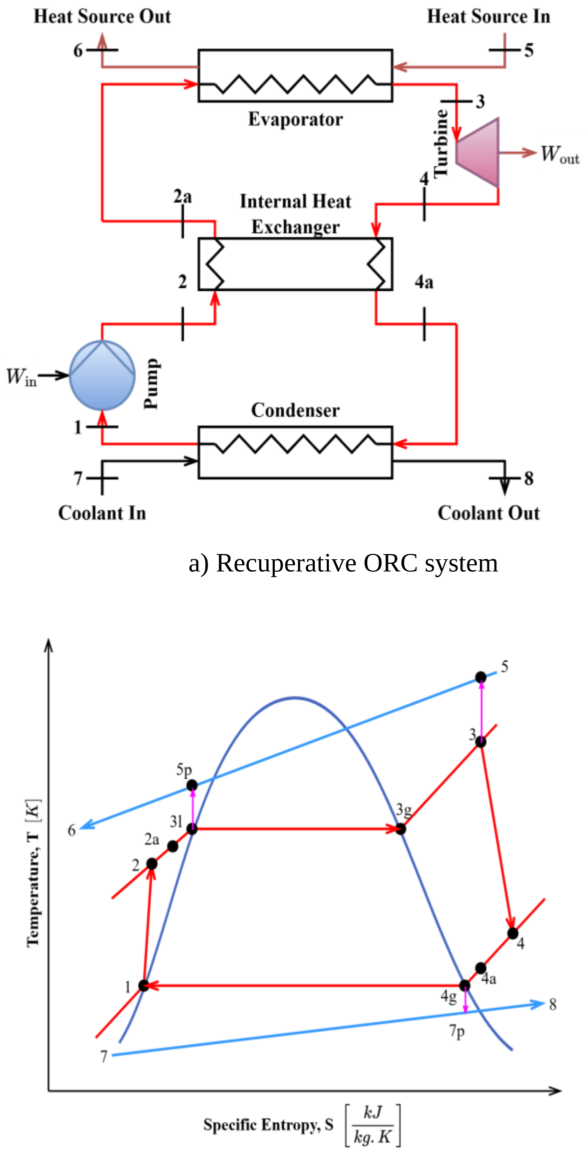

a) Recuperative ORC system

b) T-s Diagram

Fig. 2: Recuperative ORC- a) system, and b) T-s diagram

The following fundamental presumptions are made to formulate thermodynamic models: (i) steady-state operation; (ii) negligible pressure and heat losses in piping and other components other than those that are explicitly specified; (iii) kinetic and potential energy are neglected; and (iv) all components operate under adiabatic conditions, except where heat transfer is defined. The governing equations of mass, entropy, energy, and exergy balances are developed based on these assumptions. Modeled equations for pump (1→2) presented as Eq. (1-4)

$$\dot{m}_1 = \dot{m}_2 \tag{1}$$
$$\dot{m}_1 h_1 + \dot{W}_{pump} = \dot{m}_2 h_2 \tag{2}$$
$$\dot{m}_1 s_1 + \dot{S}_{g,pump} = \dot{m}_2 s_2 \tag{3}$$
$$\dot{m}_1 e_1 + \dot{W}_{pump} = \dot{m}_2 e_2 + \dot{E}_{d,pump} \tag{4}$$

Modeled equations for recuperator (2,4→2a,4a) as Eq. (5-8)

$$\dot{m}_2 + \dot{m}_4 = \dot{m}_{2a} + \dot{m}_{4a} \tag{5}$$

$$\dot{m}_2 h_2 + \dot{m}_4 h_4 = \dot{m}_{2a} h_{2a} + \dot{m}_{4a} h_{4a} \quad (6)$$
$$\dot{m}_2 s_2 + \dot{m}_4 s_4 + \dot{S}_{g,recup} = \dot{m}_{2a} s_{2a} + \dot{m}_{4a} s_{4a} \quad (7)$$
$$\dot{m}_2 e_2 + \dot{m}_4 e_4 = \dot{m}_{2a} e_{2a} + \dot{m}_{4a} e_{4a} + \dot{E}_{d,recup} \quad (8)$$

Modeled equations for evaporator (2a→3) as Eq. (9–12)

$$\dot{m}_{2a} = \dot{m}_3 \quad (9)$$
$$\dot{m}_{2a} h_{2a} + \dot{Q}_{evap} = \dot{m}_3 h_3 \quad (10)$$
$$\dot{m}_{2a} s_{2a} + \frac{\dot{Q}_{evap}}{T_{source}} + \dot{S}_{g,evap} = \dot{m}_3 s_3 \quad (11)$$
$$\dot{m}_{2a} e_{2a} + \dot{Q}_{evap}\left(1 - \frac{T_0}{T_{source}}\right) = \dot{m}_3 e_3 + \dot{E}_{d,evap} \quad (12)$$

Modeled equations for turbine (3→4) as Eq. (13-16)

$$\dot{m}_3 = \dot{m}_4 \quad (13)$$
$$\dot{m}_3 h_3 = \dot{m}_4 h_4 + \dot{W}_{turb} \quad (14)$$
$$\dot{m}_3 s_3 + \dot{S}_{g,turb} = \dot{m}_4 s_4 \quad (15)$$
$$\dot{m}_3 e_3 = \dot{m}_4 e_4 + \dot{W}_{turb} + \dot{E}_{d,turb} \quad (16)$$

Modeled equations for condenser (4a→1) as Eq. (17–20)

$$\dot{m}_{4a} = \dot{m}_1 \quad (17)$$
$$\dot{m}_{4a} h_{4a} = \dot{m}_1 h_1 + \dot{Q}_{cond} \quad (18)$$
$$\dot{m}_{4a} s_{4a} + \dot{S}_{g,cond} = \dot{m}_1 s_1 + \frac{\dot{Q}_{cond}}{T_{sink}} \quad (19)$$
$$\dot{m}_{4a} e_{4a} = \dot{m}_1 e_1 + \dot{Q}_{cond}\left(1 - \frac{T_0}{T_{sink}}\right) + \dot{E}_{d,cond} \quad (20)$$

Modeled equations for the overall system as Eq. (21-25)

$$\dot{W}_{net} = \dot{W}_{turb} - \dot{W}_{pump} \quad (21)$$
$$\dot{S}_{g,total} = \dot{S}_{g,pump} + \dot{S}_{g,recup} + \dot{S}_{g,evap} + \dot{S}_{g,turb} + \dot{S}_{g,cond} \quad (22)$$
$$\dot{E}_{d,total} = \dot{E}_{d,pump} + \dot{E}_{d,recup} + \dot{E}_{d,evap} + \dot{E}_{d,turb} + \dot{E}_{d,cond} \quad (23)$$
$$\eta_{th} = \frac{\dot{W}_{net}}{\dot{Q}_{evap}} \quad (24)$$
$$\eta_{ex} = \frac{\dot{W}_{net}}{\dot{Q}_{evap}\left(1 - \frac{T_0}{T_{source}}\right)} \quad (25)$$

2.2 Refrigerant Selection

In Organic Rankine Cycles (ORC), refrigerants act as the working fluid that transfers heat from the source to the sink. Based on their behavior in the temperature-entropy (T-s) diagram, these fluids are categorized as dry, wet, and isentropic. Wet fluids exhibit a negative vapor-line slope, which can cause condensation and potentially lead to turbine damage. Isentropic fluids have vertical vapor lines with little condensation. On the other hand, Dry fluids exhibit a positive slope by keeping the vapor superheated during expansion. Also, environmentally concerning international treaties proposed the Montreal Protocol (1987) and the Kigali Amendment (2016) for targeting nearly zero-ozone depletion potential (ODP), low-GWP refrigerants, respectively. In this study, refrigerants R1243zf, R1233zd(E), R1234ze(E), R1234yf, R1224yd(Z), and R1336mzz(Z) are selected. All of the refrigerants having a GWP (< 10) and zero ODP are shown in Table 1.

Table 1: Thermophysical properties of selected refrigerants

ASHRAE Number	P_c (MPa)	T_c (°C)	GWP (-)
R-1243zf	3.52	103.78	0.82 [12]
R-1234yf	3.38	94.70	<1 [13]
R-1234ze(E)	3.63	109.36	6 [14]
R-1224yd(Z)	3.34	155.54	1 [15]
R-1233zd(E)	3.62	166.45	<5 [16]
R-1336mzz(Z)	2.90	171.35	2 [17]

2.3 Simulation Procedure

For the present study, a flowchart of the simulation procedure is shown in Fig. 3. The simulation process begins by defining the important input parameters. This includes the thermophysical properties of the refrigerants and the temperature and pressure conditions of the source and sink fluids. After configuring the ORC modeled equations, simulations are performed sequentially for each working fluid named as R1243zf, R1234ze(E), R1234yf, R1233zd(E), R1224yd(Z), and R1336mzz(Z). For each refrigerant, evaporating and condensing pressures vary to show the effect on cycle performance. The model calculates important performance parameters such as net work, total exergy destruction, and energetic and exergetic efficiencies. Results are tabulated and shown in plots for comparison.

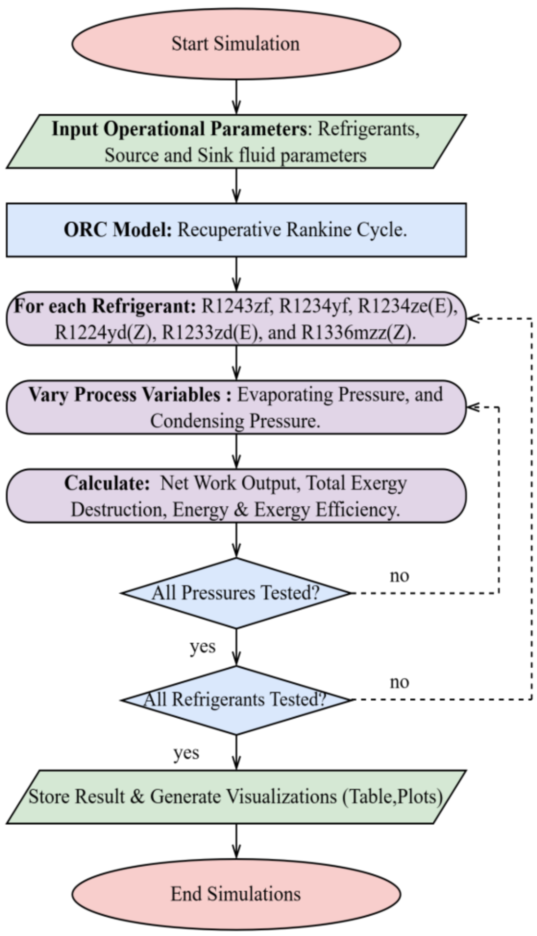

Fig. 3: Simulation procedure for the recuperative ORC

Additionally, all operational parameters for the refrigerant, hot fluid, and cold fluids used in the simulation are summarized in Table 2 and Table 3.

Table 2: Refrigerant fluid parameters used for simulation

Parameters	Unit	Recuperative ORC
Mass Flow Rate, $\dot{m}_{ref}$	kg/s	1.0
Evaporating Pressure, $P_{turb,in}$	MPa	1.0-2.0
Turbine Inlet Temperature, $T_{turb,in}$	°C	190
Condensing Pressure, $P_{pump,in}$	MPa	0.8-1.5
Temperature difference, $\Delta T_{recup}=T_{3l}-T_{2a}$	°C	10
Pump Isen. Efficiency, $\eta_{pump,isen}$	--	0.9
Turbine Isen. Efficiency, $\eta_{turb,isen}$	--	0.9

Table 3: Evaporator and Condenser fluid known parameters

Parameters	Unit	Recuperative ORC
Evaporator (Hot Fluid)	--	Air
Evap. Inlet Pressure ($P_{evap,in}$)	kPa	101.325
Evap. Inlet Temperature ($T_{evap,in}$)	°C	220
Evap. Outlet Pressure ($P_{evap,out}$)	kPa	101.325
Evap. PPTD ($\Delta T_{evap,pinch}$)	K	5
Condenser (Cold Fluid)	--	Air
Cond. Inlet Pressure ($P_{cond,in}$)	kPa	101.325
Cond. Outlet Pressure ($P_{cond,out}$)	kPa	101.325
Cond. Inlet PPTD ($\Delta T_{cond,in,pinch}$)	K	8
Cond. PPTD ($\Delta T_{cond,pinch}$)	K	5
Dead State Temperature (T_0)	K	288.15

3. Result and Discussion

In this section, the effect of evaporating (1.0 - 2.0 MPa) and condensing (0.8 - 1.5 MPa) pressure on the performance parameters (total exergy destruction, net work output, thermal efficiency, and exergetic efficiency) of the recuperative ORC will be investigated.

3.1 Effect of Evaporating Pressure

Fig. 4 and Fig. 5 show the variation of evaporating pressure (P_3) on net work output ($\dot{W}_{out}$) and total exergy destruction ($\dot{E}_{dest}$), respectively. In this recuperative ORC, $\dot{W}_{out}$ steadily increases with P_3, since increasing P_3 refers to the enhancement of the pressure ratio in the turbine, which facilitates a greater drop in enthalpy and therefore larger work output from the turbine. On the other hand, total exergy destruction ($\dot{E}_{dest}$) decreases with the rise of evaporating pressure (P_3), which reflects the reduction of irreversibilities in heat transfer and expansion processes at elevated pressures. R-1243zf achieves the highest net power (28.04 kW at 2.0 MPa) with moderate exergy destruction (48.66 kW). R-1234yf and R-1234ze(E) provide balanced performance, while R-1224yd(Z) shows a lower exergy destruction (16.76 kW), and R-1336mzz(Z) only **14.28 kW** net work out at maximum pressure.

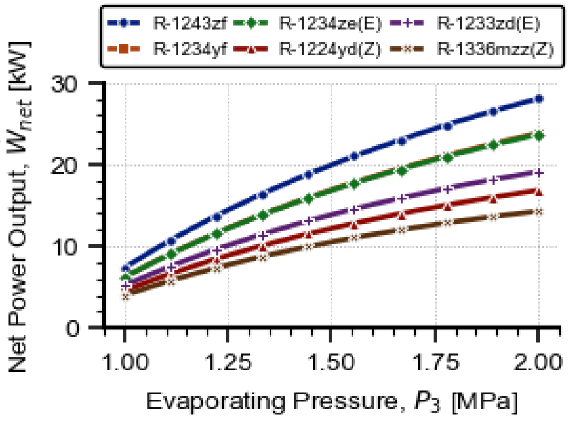

Fig. 4: Effect of evaporative pressure on net power output

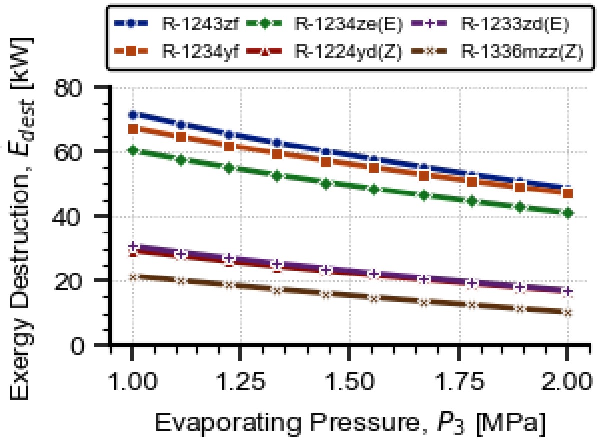

Fig. 5: Effect of evaporating pressure on exergy destruction

Besides the net work and the total exergy destruction, the variation of energy (η_{en}) and exergy efficiency (η_{ex}) due to evaporating pressure (P_3) is shown in Fig. 6 and Fig. 7. Both efficiencies are increasing with increasing evaporating pressure for all six low-GWP refrigerants. Since higher evaporation pressure facilitates larger net work output from the system, which indicates greater efficiencies according to Eq. (24) and Eq. (25). In terms of thermal efficiency, R-1243zf demonstrates a superior thermal efficiency of **9.43%** and an exergetic efficiency of **31.00%** at 2.0 MPa. While R-1224yd(Z) shows comparable energy efficiency at **9.48%**, its exergetic efficiency of **27.08%**.

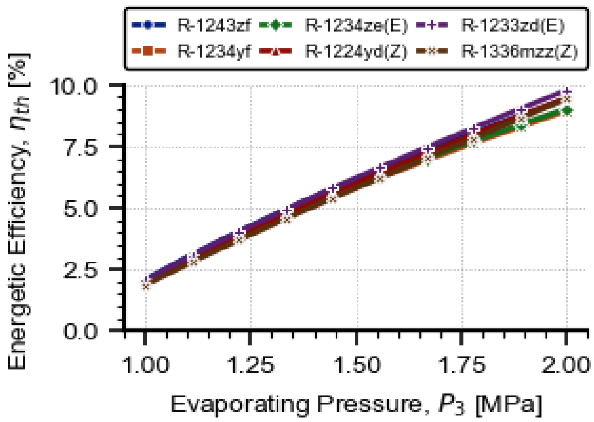

Fig. 6: Effect of evaporative pressure on energy efficiency

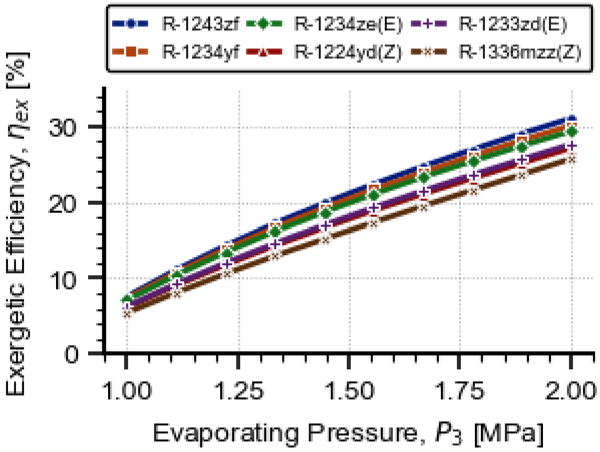

Fig. 7: Effect of evaporative pressure on exergy efficiency

3.1 Effect of Condensing Pressure

Fig. 8 and Fig. 9 show the variation of total exergy destruction ($\dot{E}_{dest}$) and net power output ($\dot{W}_{out}$) for the change of condensing pressure (P_1). Due to the reduction of the pressure ratio leading to lower turbine work output for the increase of condensing pressure (P_1). Among the six refrigerants, **R-1243zf** shows the highest net power (28.04 kW at 0.8 MPa), followed by **R-1234yf** and **R-1234ze(E)**, while **R-1224yd(Z)**, **R-1233zd(E)**, and **R-1336mzz(Z)** perform lower.

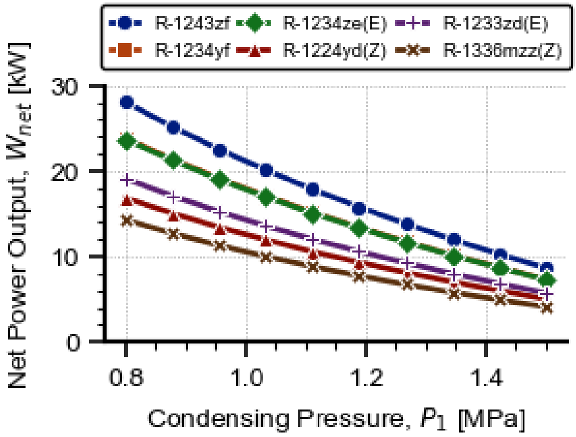

Fig. 8: Effect of condensation pressure on net power output

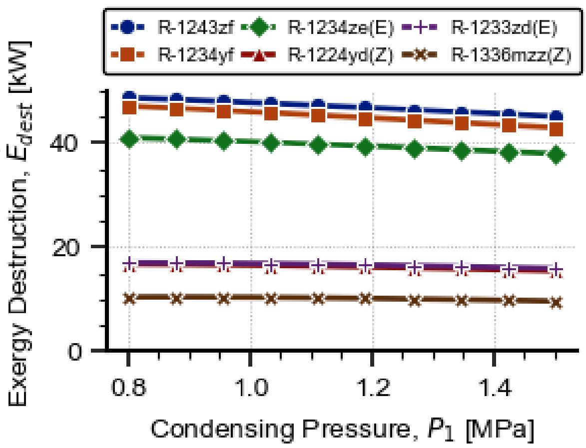

Fig. 9: Effect of condensing pressure on exergy destruction

Also, the energy (η_{en}) and exergy efficiency (η_{ex}) of the system drop with the rise of condensing pressure (P_1), shown in Fig. 10 and Fig. 11. Since a higher condensing pressure makes a smaller pressure ratio in the turbine inlet and outlet. As a result, less power is extracted from the turbine, which results in less energy and exergy efficiency according to Eq. (24) and Eq. (25). At the lowest pressure (0.8 MPa), the refrigerants rank as follows: R-1233zd(E) achieves the maximum at 9.79%, followed by R-1234ze(E) at 9.04%, R-1224yd(Z) at 9.48%, R-1243zf at 9.43%, R-1234yf at 8.94%, and R-1336mzz(Z) showing the minimum at 9.43%. On the other hand, R-1243zf delivers the maximum exergy efficiency at 31.0%, R-1234yf at 30.0%, R-1234ze(E) at 29.3%, R-1233zd(E) at 27.6%, R-1224yd(Z) at 27.1%, and R-1336mzz(Z) shows the minimum at 25.7%.

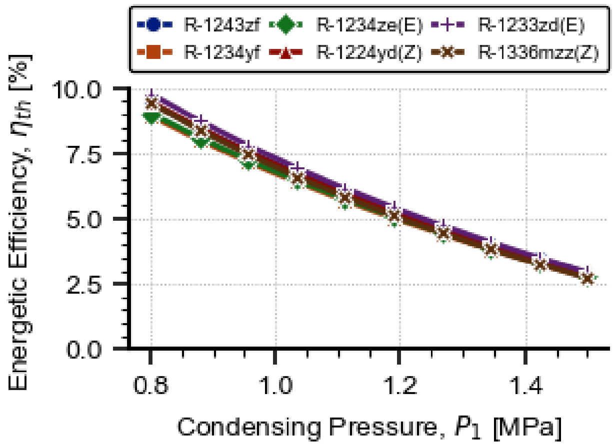

Fig. 10: Effect of condensing pressure on energy efficiency

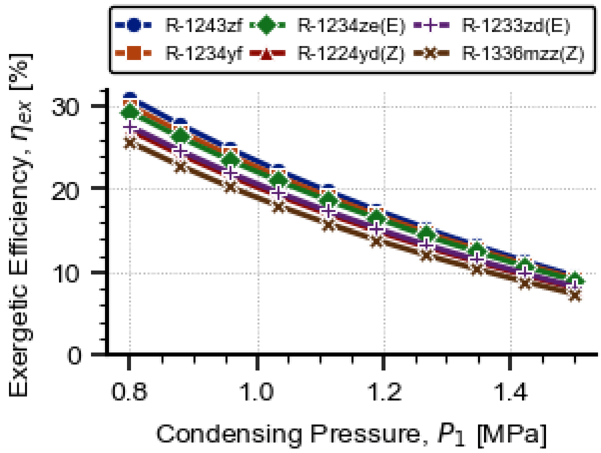

Fig. 11: Effect of condensing pressure on exergy efficiency

4. Conclusion

This study comprehensively studied the energy and exergy performance of recuperative ORC for six low GWP (<10) refrigerants (R1234yf, R1243zf, R1224yd(Z), R1234ze(E), R1233zd(E), and R1336mzz(Z)). At optimal conditions (P_3=2.5 MPa, P_1=0.8 MPa), R-1243zf emerges as the optimal refrigerant choice for recuperative ORC systems, offering the best combination of high power output (**28.04 kW**), excellent thermal efficiency (**9.43%**), and superior exergetic efficiency (**31.00%**), making it most suitable for applications prioritizing maximum power generation. R-1243zf leads in performance, followed by R-1234yf and R-1234ze(E). Whereas R-1233zd(E) shows the highest thermal efficiency (**9.78%**), R-1224yd(Z) performs moderately, and

R-1336mzz(Z) ranks lowest in exergetic efficiency with minimal irreversibilities.

5. References

[1] A. O. Ochieng, T. F. Megahed, S. Ookawara, and H. Hassan, "Comprehensive review in waste heat recovery in different thermal energy-consuming processes using thermoelectric generators for electrical power generation," *Process Safety and Environmental Protection*, vol. 162, pp. 134–154, June 2022.

[2] C. Ononogbo, E. Nwosu, N. Nwakuba, G. Nwaji, O. Nwufo, O. Chukwuezie, M. Chukwu, and E. Anyanwu, "Opportunities of waste heat recovery from various sources: Review of technologies and implementation," *Heliyon*, vol. 9, no. 2, p. e13590, Feb. 2023.

[3] S. O. Oyedepo and B. A. Fakeye, "WASTE HEAT RECOVERY TECHNOLOGIES: PATHWAY TO SUSTAINABLE ENERGY DEVELOPMENT," *Journal of Thermal Engineering*, vol. 7, no. 1, pp. 324–348, Jan. 2021.

[4] C. E. Sprouse, "Review of Organic Rankine Cycles for Internal Combustion Engine Waste Heat Recovery: Latest Decade in Review", *Sustainability*, vol. 16, no. 5, p. 1924, Feb. 2024.

[5] A. Javanshir, N. Sarunac, and Z. Razzaghpanah, "Thermodynamic Analysis of ORC and Its Application for Waste Heat Recovery," *Sustainability*, vol. 9, no. 11, p. 1974, Oct. 2017.

[6] H. Fang, J. Xia, K. Zhu, Y. Su, and Y. Jiang, "Industrial waste heat utilization for low temperature district heating," *Energy policy*, vol. 62, pp. 236–246, 2013.

[7] X. Hu, T. Ma, S. Dong, C. Zhang, W. Zhuang, and T. Zhang, "Design and selection of working fluids for ORC system using computer-aided molecular design and group contribution method," *Applied Thermal Engineering*, vol. 274, p. 126593, Sept. 2025.

[8] M. Bahrami, F. Pourfayaz, and A. Kasaeian, "Low global warming potential (GWP) working fluids (WFs) for Organic Rankine Cycle (ORC) applications," *Energy Reports*, vol. 8, pp. 2976–2988, Nov. 2022.

[9] B. Tan, Z. Wang, J. Huang, Z. Xiao, K. Zhang, and Y. Xiao, "Experimental study of ORC-VCR system using low-GWP fluid R1233zd(E)," *Thermal Science and Engineering Progress*, vol. 66, p. 104085, Oct. 2025.

[10] F. Tanbar, R. Febriyanto, H. M. Ariyadi, A. D. Nugraha, A. A. Simaremare, E. Supriyanto, M. Triani, and M. A. Muflikhun, "Techno-economic studies of low GWP-organic Rankine cycle for low-level geothermal waste heat utilization in Remote Island of Indonesia," *Case Studies in Thermal Engineering*, vol. 65, p. 105385, Jan. 2025.

[11] Y. Jiang, X. Zhang, Z. Zhang, L. Hao, Z. Cao, S. Li, B. Guo, Y. Zheng, C. Dong, and L. Zhao, "Performance Evaluation and Working Fluid Screening of Direct Vapor Generation for Solar ORC Using Low-Global Warming Potential (GWP) Working Fluids," *Energies*, vol. 17, no. 13, p. 3133, June 2024.

[12] B. Sheng, Z. Li, W. Liu, X. Chen, Y. Zhao, X. Dong, H. Yan, J. Shen, and M. Gong, "The isochoric special heat capacity for 3, 3, 3-trifluoroprop-1-ene (R1243zf) at temperatures from (299 to 351) K and pressures up to 11 MPa," *The Journal of Chemical Thermodynamics*, vol. 153, p. 106319, 2021.

[13] Ø. Hodnebrog, B. Aamaas, J. S. Fuglestvedt, G. Marston, G. Myhre, C. J. Nielsen, M. Sandstad, K. P. Shine, and T. J. Wallington, "Updated global warming potentials and radiative efficiencies of halocarbons and other weak atmospheric absorbers", *Reviews of Geophysics*, vol. 58, no. 3, p. e2019RG000691, 2020.

[14] S. Fukuda, C. Kondou, N. Takata, and S. Koyama, "Low GWP refrigerants R1234ze (E) and R1234ze (Z) for high temperature heat pumps," *International journal of Refrigeration*, vol. 40, pp. 161–173, 2014.

[15] R. Akasaka and E. W. Lemmon, "A Helmholtz Energy Equation of State for cis-1-Chloro-2, 3, 3, 3-tetrafluoro-1-propene [R-1224yd (Z)]," *International Journal of Thermophysics*, vol. 44,no.11, p. 166, 2023.

[16] R. J. Hulse, R. S. Basu, R. R. Singh, and R. H. P. Thomas, "Physical properties of HCFO-1233zd (E)," *Journal of chemical & engineering data*, vol. 57, no. 12, pp. 3581–3586, 2012.

[17] S. Wang, Z. Guo, X. Han, X. Xu, Q. Wang, S. Deng, and G. Chen, "Experimental evaluation on low global warming potential HFO-1336mzz-Z as an alternative to HCFC-123 and HFC-245fa," *Journal of Thermal Science and Engineering Applications*, vol. 11, no. 3, p. 031009, 2019.

6. Nomenclature

Symbol	Meaning	Unit
T	Temperature	K
P	Pressure	Pa
h	Specific Enthalpy	kJ/kg
s	Specific Entropy	kJ/kgK
e	Specific Exergy	kJ/kg
$\dot{m}$	Mass Flow Rate	kg/s
$\dot{Q}$	Heat Transfer Rate	kJ/s
MBE	Mass Balance Equation	-
EBE	Energy Balance Equation	-
EnBE	Entropy Balance Equation	-
ExBE	Exergy Balance Equation	-
WHR	Waste Heat Recovery	-
GWP	Global Warming Potential	-
ODP	Ozone Depletion Potential	-
HFOs	Hydrofluoroolefins	-
RORC	Recuperative Organic Rankine Cycle	-
EES	Engineering Equation Solver	-
VCR	Vapor compression refrigeration	-